



ESR and ESR/U-series chronology of the Middle Pleistocene site of Tourville-la-Rivière (Normandy, France) - A multi-laboratory approach

Jean-Jacques Bahain^{a,*}, Mathieu Duval^{b,c}, Pierre Voinchet^a, Hélène Tissoux^{a,d,e},
Christophe Falguères^a, Rainer Grün^b, Davinia Moreno^c, Qingfeng Shao^f, Olivier Tombret^a,
Guillaume Jamet^g, Jean-Philippe Faivre^h, Dominique Cliquetⁱ

^a UMR 7194 HNHP, Muséum National d'Histoire Naturelle, Département Homme et Environnement, 1 rue René Panhard, 75013, Paris, France

^b Australian Research Centre for Human Evolution (ARCHE), Environmental Futures Research Institute, Griffith University, NATHAN QLD, 4111, Australia

^c Geochronology, Centro Nacional de Investigación sobre la Evolución Humana (CENIEH), Paseo Sierra de Atapuerca, 3, 09002, Burgos, Spain

^d BRGM, DGR/GAT, 3 Avenue Claude Guillemin, BP 36009, 45060, Orléans, France

^e UMR7194 HNHP, France

^f Nanjing Normal University, College of Geography Science, Nanjing, China

^g GéoArchéon SARL, 30, rue de la Victoire, F-55210 Viéville-sous-les-Côtes, France & Laboratoire de Géographie Physique Environnements quaternaires et actuels (UMR 8591, CNRS-Universités Paris I & Paris XII), 1 place Aristide Briand, F-92195 Meudon cedex, France

^h Université de Bordeaux, PACEA, UMR 5199, F-33615, Pessac Cedex, France

ⁱ Service Régional de l'Archéologie, Direction régionale des Affaires culturelles de Basse-Normandie, 13bis, rue de Saint-Ouen, 14052, Caen cedex 04 & UMR CNRS 6566, Université de Rennes 1, France

ARTICLE INFO

Keywords:

Electron Spin Resonance (ESR) dating
Combined ESR/U-series dating
Tourville-la-Rivière
Middle Pleistocene
Teeth
Optically bleached quartz grains

ABSTRACT

– Tourville-la-Rivière (Normandy, France) is one of the rare Middle Pleistocene palaeoanthropological localities of Northern France. Electron Spin Resonance (ESR) and combined ESR/U-series dating methods were independently applied by different teams on sediments and teeth from this site. The present work provides an overview of this multi-laboratory dating work by integrating a description and discussion of the methodologies employed and results obtained.

Results confirm that the ESR/U-series analyses of the teeth are greatly dependent on the U-uptake histories of the dental tissues. Although all teeth come from the same archeological level, the samples analysed by each team display two different patterns for the U-series data. This is most likely related to the different sampling areas selected by each team and may be interpreted as the result of local variations in the geochemical conditions of the surrounding environment. Concerning the ESR dating of optically bleached quartz grains, the use of the multiple centre approach seems crucial when dating such fluvial and fluvio-lacustrine sediments. Our results also confirm the great potential of the Ti-H centre to date late Middle Pleistocene deposits.

Despite some (expected) discrepancies related to the independent use of parameters and approaches by the different teams involved in this multi-laboratory study, the whole ESR and ESR/U-series data set collected from Tourville-la-Rivière locality consistently correlates stratigraphic levels D1 to I and associated human occupation to MIS7.

1. Introduction

Since the late 1980s, Electron Spin Resonance (ESR) of optically bleached quartz grains and combined ESR/U-series of fossil teeth are amongst the most employed dating applications to constrain the chronology of Middle Pleistocene archaeo-palaeontological sites.

Previous cross-comparison studies showed good agreement with results derived from other numerical dating methods such as Luminescence, U-series and ⁴⁰Ar-³⁹Ar (e.g. Duval et al., 2017; Méndez-Quintas et al., 2018; Pereira et al., 2018). Unfortunately, given the very limited number of laboratories and researchers specialized in the ESR dating applications mentioned above, inter-laboratory comparison studies

* Corresponding author.

E-mail addresses: bahain@mnhn.fr (J.-J. Bahain), m.duval@griffith.edu.au (M. Duval), pvoinchet@mnhn.fr (P. Voinchet), h.tissoux@brgm.fr (H. Tissoux), falguere@mnhn.fr (C. Falguères), rainer.grun@griffith.edu.au (R. Grün), davinia.moreno@cenieh.es (D. Moreno), qingfengshao@nynu.edu.cn (Q. Shao), olivier.tombret@mnhn.fr (O. Tombret), guillaume.jamet@geoarcheon.fr (G. Jamet), jean-philippe.faivre@u-bordeaux.fr (J.-P. Faivre), dominique.cliquet@culture.gouv.fr (D. Cliquet).

<https://doi.org/10.1016/j.quaint.2019.06.015>

Received 30 July 2018; Received in revised form 15 March 2019; Accepted 11 June 2019

Available online 15 June 2019

1040-6182/ © 2019 Elsevier Ltd and INQUA. All rights reserved.

remain very rare. Additionally, the material analyzed is typically quite small and heterogeneous, which does not facilitate the implementation of such large-scale comparative programs.

Sometimes, a given site or archaeological level has been dated with ESR or ESR/U-series methods by different teams in separate works, such as for example the sites of La Micoque (Dordogne, France) (Schwarcz and Grün, 1988; Falguères et al., 1997) or Atapuerca Gran Dolina TD6 (Spain) (Falguères et al., 1999; Duval et al., 2018) or, more rarely, within the framework of a single study (e.g. Dirks et al., 2017). However, except for critical evaluations of previously published data, these studies have in most cases not led to any proper scientific discussions about the experimental conditions employed and their impact on the final age estimates.

Tourville-la-Rivière is one of the rare Middle Pleistocene palaeoanthropological localities of Northern France. It has recently been submitted to a series of independent dating studies by different ESR dating laboratories (CENIEH-RSES, MNHN and BRGM) involving combined ESR/U-series dating of fossil teeth (CENIEH-RSES in Faivre et al., 2014; MNHN in Bahain et al., 2015) and ESR dating of optically bleached quartz grains (MNHN and BRGM, unpublished data). The present paper aims to compile all the chronological data collected for this site in order to enable a proper comparison of the different methodologies employed (from sampling to age determination) and evaluate their impact on the age results. When necessary, new age calculations were performed in accordance to recent methodological developments. These data will contribute to refine the chronology of the different archaeological and geological levels for this key palaeoanthropological locality.

2. Tourville-La-Rivière site

Located on a low fossil fluvial terrace of the Seine System, close to Rouen city in Normandy (Fig. 1), Tourville-la-Rivière site (Seine-Maritime, France) has been known since the late 1960s (see Lautridou, 1985 and Jamet, 2015 and references therein). Several areas within the site have been successively excavated during the following fifty years, delivering an abundant late Middle Pleistocene mammal fauna (Auguste, 2009; Bemilli, 2010, 2014), a rich archaeological Middle Paleolithic lithic assemblage (Cliquet, 2010; Faivre et al., 2014) and three human arm bones attributed to an individual of the Neanderthal lineage (Faivre et al., 2014).

Tourville-la-Rivière offers one of the longest Middle Pleistocene continental stratigraphic sequences (> 30 m thick) in Western Europe (Lautridou, 1985) (Fig. 2). At least two climatic cycles are recorded on a fluvial terrace level corresponding to the T2 terrace of the Seine system (Fig. 1). The lower part of the sequence (units A-D) consists of periglacial coarse sands and gravels units with intercalations of fine-grained interglacial fluvial or estuarine sediments. The upper part (units E to J) corresponds to successions of fine-grained sediments, gravels and paleosols, covered by periglacial slope deposits (units K and L) (Lautridou, 1985; Jamet, 2015; Chauhan et al., 2017). Chronological data available before 2014 (ESR on mollusk shells, Stremme, 1985; Amino acid racemization (AAR) also on mollusk shells, Occhietti et al., 1987; Thermoluminescence (TL) and Infra-red stimulated luminescence (IRSL) on sediments, Balescu et al., 1997; see data in Fig. 2) correlated the fluvial and estuarine deposits to the Saalian stage and place the deposition of units B and D1 during MIS 9 and 7, respectively.

The locality has recently been the subject of two successive archaeological excavation campaigns in 2008 (Cliquet, 2010) and 2010 (Faivre et al., 2014) and a new stratigraphic study was performed within the framework of Guillaume Jamet's PhD thesis (Jamet, 2015). The latter enabled to propose that the position of the end of the MIS7 is recorded higher up in the sequence, i.e. between units E and F instead of between D1 and D2 as previously proposed by Lautridou (1985) (Fig. 2).

3. Electron spin resonance (ESR) dating: basic principles

3.1. Combined ESR/U-series dating of fossil teeth

The combined use of electron spin resonance (ESR) and U-series dating methods (ESR/U-series) to date Pleistocene mammal remains has been first proposed at the end of 1980s (Grün et al., 1988). The age calculation for a tooth requires the determination of two parameters: an estimate of the total dose of radiation received during its archaeological history, usually named equivalent dose (D_e), and the dose rate (d_a), i.e. an estimate of the dose annually absorbed by the sample. The D_e value is classically determined using a multiple aliquot additive dose (MAAD) method. The dose rate is assessed from the radioelement content of the sample itself and of the surrounding sediment, in addition to a component from the cosmic rays (see Duval, 2015 for further detail).

The main complication in combined ESR/U-series dating of fossil teeth is related to the uranium incorporation into dental tissues during the fossilization process. This phenomenon depends on the considered tissue, of the geological nature of the site and of its age. It requires the use of mathematical models allowing the description of the U-content evolution with time in a given tissue. The most popular one, uranium-series (US) model, has been proposed by Grün et al. (1988), who introduced a parameter (p) to describe the U-uptake kinetics for each dental tissue. This kinetics is mathematically assessed from the ESR and present-day U-series data measured in each dental tissue. Consequently, only one combined US-ESR age fits the available dataset (see Shao et al., 2015 for the mathematical basis of the US model).

The US model can only be applied if the ESR age calculated assuming an early U-uptake (EU) for all the tissues of a tooth is greater than the corresponding EU-U-series ages. In other words, the occurrence of U-leaching would preclude the use of the US model, which may frequently occur in Pleistocene open air sites. More recently, Shao et al. (2012) proposed the accelerated uptake (AU) model in order to enable combined U-series/ESR age calculations in presence of uranium leaching.

Another alternative to the US model is the closed system uranium-series (CSUS or CSUS-ESR) model that assumes that all uranium migrated into the dental tissue at the time given by the apparent closed system U-series age (Grün, 2000a). On a given data set, the CSUS model typically provides a maximum possible age estimate. By using both CSUS and US models for a given sample, the resulting age range typically encompass all possible U-uptake histories (e.g. Duval et al., 2018), as long as there are no U-leaching episodes.

3.2. ESR dating of optically bleached quartz grains

Unlike for fossil teeth, ESR dating of quartz grains is based on the evaluation of light-sensitive signals. The exposure of quartz grains to natural sunlight (and especially to UV-rays; Tissoux et al., 2007) leads to the significant decrease of the intensity associated to the ESR signal of some paramagnetic centres. This phenomenon, called optical bleaching, corresponds to a drain of trapped electrons in relation to the energy received during the light exposure (Toyoda et al., 2000). Hence, the event tentatively dated here is not the crystal formation, as for the speleothems, or a biological event, as for palaeontological remains, but the last exposure of the quartz grains to the sunlight before their burial into the sediment (Yokoyama et al., 1985).

However, the different ESR centres measured in quartz do not all show the same bleaching features. If the ESR intensity of the titanium (Ti) centres (mainly Ti-H and Ti-Li) can be fully reset, the aluminium (Al) signal cannot be zeroed. Instead its ESR intensity decreases until a plateau value corresponding to the presence in the quartz of traps that cannot be emptied by light exposure (Toyoda et al., 2000; Tissoux et al., 2012). This residual value is sample dependent: it is typically determined by exposing an aliquot of the natural sample to a UV solar simulator (e.g. Voinchet et al., 2003). The ESR intensity corresponding

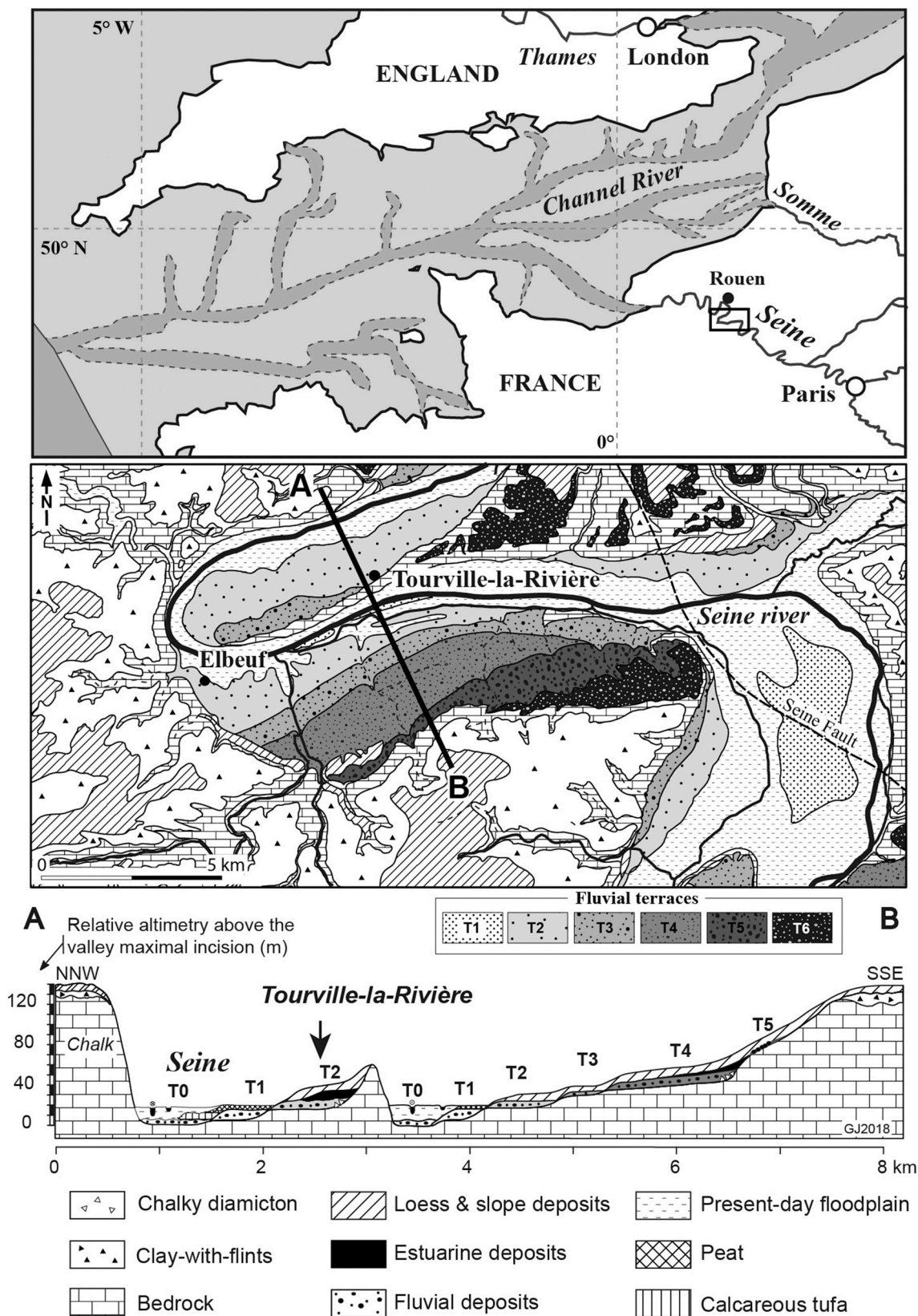


Fig. 1. Location of the Tourville-la-Rivière site, Northern France, in the Seine valley terrace system (after Jamet, 2015).

to the non-bleachable part of the ESR AI signals is then subtracted to the corresponding ESR signal intensity of the studied sample before any D_e determination (so-called total bleach method, Forman et al., 2000). The resulting D_e value corresponds to the total dose of radiation received by

the sample during burial (Voinchet et al., 2004).

In order to evaluate the bleaching level achieved by the ESR signals during sediment transport, an approach based on the measurements of AI and T1 signals (multiple centre approach, MC) was first proposed by

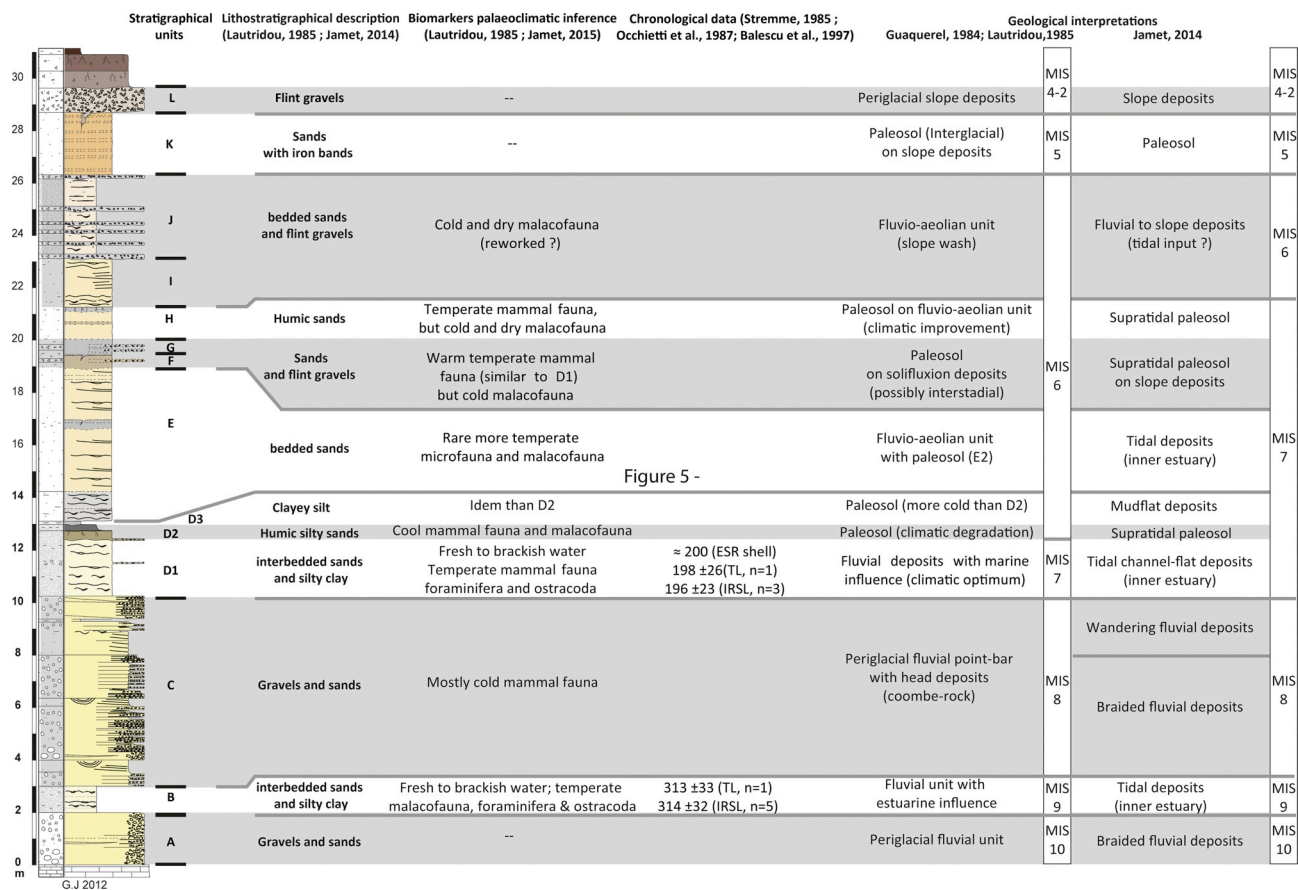


Fig. 2. Overview of the sedimentary sequence at Tourville-la-Rivière, including stratigraphic subdivision, biomarkers identified, numerical dating results available before the recent ESR/U-series and ESR studies, and palaeoenvironmental interpretation (after Jamet, 2015).

Toyoda et al. (2000). This MC approach aims to take advantage of the different bleaching kinetics typically observed for the Al, Ti-Li and Ti-H centres. The Ti-H signal is known to be fully reset at a much faster rate than the Ti-Li signal, while the Al signal shows a much slower bleaching kinetics in comparison (Toyoda et al., 2000; Duval et al., 2017). Incomplete bleaching would therefore lead to different burial dose estimates for these three ESR signals, with the Ti-H signal typically providing the smallest dose and the Al signal the biggest one. In this case, the first one would most likely be the closest estimate of the true burial dose absorbed by the sample, whereas the second one would provide a maximum possible estimate (see Duval et al., 2017). However, the systematic application of the MC approach is sometimes complicated by the weak ESR signal measured for the Ti-H centre (see Rixhon et al., 2017), which makes it complicated to obtain meaningful results.

A few recent applications studies may provide a fair idea of the time range applicability achieved by the MC approach. Ti-H signal has proven to produce age estimates consistent with independent age control from about 300 ka to 40 ka (e.g., Duval et al., 2017; Kreutzer et al., 2018), while Ti-Li and Al centres may provide accurate age results between about 200 ka and 2 Ma (Beerten and Stesmans, 2006; Méndez-Quintas et al., 2018; Sahnouni et al., 2018; Voinchet et al., this issue). For a time period younger than about 40 ka, none of the Al and Ti centres seem to yield accurate age results (e.g., Méndez-Quintas et al., 2018), which indicate the difficulty to detect low dose estimates (< 100 Gy) with these signals. Finally, one may not exclude that the lower dating limit of the ESR method may well be beyond 2 Ma, as suggested in first instance by the few existing thermal stability studies (see an overview in Toyoda, 2015). However, it is still unclear whether these laboratory estimates are accurate given the uncertainty involved in the evaluation process and the impossibility to reproduce natural

condition during annealing experiments.

4. Material and methods

4.1. Combined ESR/U-series dating of fossil teeth

Eight fossil teeth from the 2010 excavation (Fig. 3) were analyzed by the CENIEH-RSES (Centro Nacional de Investigación sobre la Evolución Humana, Spain – Research School of Earth Sciences, Australian National University, Australia) team (see details in Faivre et al., 2014): five of them were found in the lower part of Layer D2 (T1, T2, T4, T5 and T8) and three in the upper part (T3, T6 and T7). Four sediment samples were collected from Layer D2, with three in direct contact with T4, T5 and T7. They were used to derive the external beta and gamma dose rate values. Since the dating analyses started at the end of 2011, i.e. more than one year after the end of the excavation (September 2010), the excavation site could no longer be accessed to carry out *in situ* gamma dose rate measurements.

Six horse teeth from the D2 level excavated in 2008 and associated sediments (Fig. 3) have been analyzed by the MNHN (Muséum National d'Histoire Naturelle, France) team following the experimental protocol described in Bahain et al. (2012). *In situ* gamma dose rate evaluation was also performed in 2011 on an outcrop connecting the two main excavation areas. Four measurements were performed within D2 layer in order to evaluate lateral variations of radioactivity.

The analytical protocols followed by the two teams are summarized in Table 1. They are quite similar for the sample preparation and D_e determination, but differ for the U-series analyses and some of the ESR parameters used in the age calculation. The main differences may be summarized as follows: (i) external dose rate was determined from

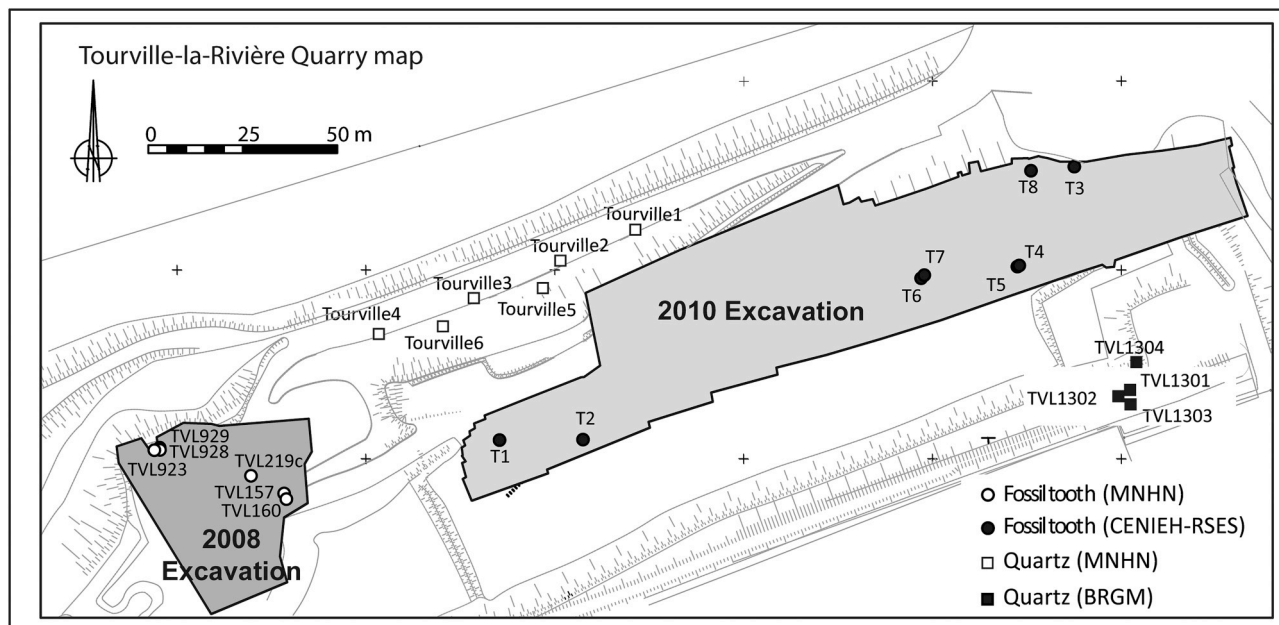


Fig. 3. Sampling location or the analyzed teeth and sediments from the Tourville-la-Rivière site.

laboratory analyses of sediment only for CENIEH-RSES tooth samples, while gamma dose rate of the MNHN samples was derived from *in situ* measurements; (ii) Potential Rn losses from the dental tissues was evaluated for the MNHN samples, while equilibrium was assumed for the CENIEH-RSES teeth; (iii) the cosmic dose rate was estimated from the present-day depth by CENIEH-RSES team (i.e.21m, leading to a cosmic dose of 26.8 $\mu\text{Gy/a}$), while MNHN used a geological model based on the sediment deposition interpretation from [Jamet \(2015\)](#)

(leading to a mean cosmic dose of about 100 μGy); (iv) the dose rate conversion factors from [Adamic and Aitken \(1998\)](#) and [Guérin et al. \(2011\)](#) were used by MNHN and CENIEH-RSES teams, respectively; (v) DATA (CENIEH-RSES)([Grün, 2009](#)) and USESR (MNHN)([Shao et al., 2015](#)) combined ESR/U-series age calculation programs were employed.

Table 1

Comparison of the analytical procedures used by the CENIEH-RSES and MNHN teams for the combined U-series/ESR dating of fossil teeth.

Analytical steps	CENIEH-RSES	MNHN
<i>Preparation</i>	Mechanic with dentist drill	
<i>Selected grain size</i>	100–200 μm	
<i>Impact of preparation on alpha and beta dose rate</i>	Data from Marsh (1999)	Data from Brennan et al. (1997)
<i>Number of dose irradiation steps</i>	10	
<i>Maximum irradiation dose (D_{max})</i>	5,000 Gy	
<i>Measurement of the ESR intensity</i>	Peak-to-peak amplitude (T1B2; Grün, 2000b)	
<i>Fitting function - data weighting</i>	Single Saturating Exponential (SSE) – Inverse of the squared ESR intensities ($1/I^2$)	
<i>Fitting program</i>	Origin	
<i>U-series analyses of dental tissues</i>	High resolution Laser Ablation ICP-MS analyses (as in Grün et al., 2014) The U-series data from all the laser ablation spots of a given tissue were combined to provide the data input for the ESR age calculations	Solution alpha spectrometry bulk analyses
<i>Alpha efficiency</i>	0.13 \pm 0.02 (Grün and Katzenberger-Apel, 1994)	
<i>Rn loss in dental tissues</i>	Equilibrium was assumed	Determined by cross-checking data from High resolution gamma spectrometry (HRGS) and alpha spectrometry analyses (Bahain et al., 1992)
<i>Water content of dental tissues</i>	Enamel = 0% wgt Dentine = 5 \pm 3% wgt	Enamel = 0% wgt Dentine = 7 \pm 5% wgt
<i>Radioelement contents in sediment</i>	Determined by ICP-MS/OES The values were used to derive the beta and gamma dose rates	Determined by HRGS The values were used to derive the beta dose rates
<i>Water content of sediment</i>	20 \pm 10% wgt	15 \pm 5% wgt
<i>Dose rate conversion factors</i>	Guérin et al. (2011)	Adamic and Aitken (1998)
<i>In situ gamma measurements</i>	No (gamma dose rate calculated from radioelement contents)	Yes (NaI probe connected to a Inspector1000 Canberra multichannel analyzer) on a section close to the excavation area. Gamma dose rates were obtained with the Threshold method (Mercier and Falguères, 2007). A mean gamma dose rate was derived from the 4 <i>in situ</i> measurements performed within layer D2.
<i>Cosmic dose rate</i>	Calculated from present-day depth (according with the tables of Prescott and Hutton, 1988, 1994)	Calculated using a three stage model evolution based on Jamet's geological interpretation (according with the tables of Prescott and Hutton, 1988, 1994)
<i>Age calculation program</i>	DATA program (US-ESR and CS-USESR ages) (Grün, 2009)	USESR (US, Shao et al., 2014) and DATA (CS-US, Grün, 2009) programs

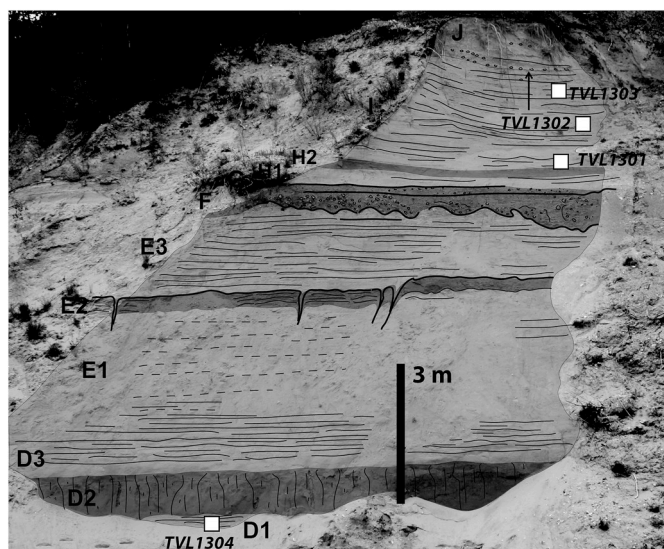


Fig. 4. Sampling location of the 2013 sediments from Tourville-la Rivière analyzed by the BRGM team.

4.2. ESR dating of quartz grains

Six sediment samples were collected in 2011 at Tourville-la-Rivière, two from the D1 level (Tourville 5 & 6) and another four from the D2 level (Tourville 1 to 4). These last four samples actually correspond to the *in situ* gamma measurement points used for the MNHN teeth (Fig. 3). *In situ* gamma measurements were systematically performed at each sampling point using an Inspector1000 Canberra gamma spectrometer. Gamma dose rate were obtained using the threshold approach. By this approach, the count-rate of the spectrometer, proportional to the gamma dose-rate, is directly determined independently of the radioelements sources (U, Th, K) (see details in Mercier and Falguères, 2007).

Four sediment samples were collected by the BRGM (Bureau de Recherche Géologique et Minière, France) team in 2013 (TVL1301 to 04) from one new section cleaned and studied by Guillaume Jamet during his PhD (Fig. 4), located approximately 150m ESE from the MNHN sampling section (Fig. 3). One sample was taken from the D1 level (TVL1304) and the other three from I level. Here again, *in situ*

gamma spectrometry measurements were systematically performed using an Ortec Digidart LF gamma spectrometer and gamma dose rates derived from the threshold approach.

The two teams employed the same preparation and measurement procedure. Quartz grains were extracted using physical and chemical preparation techniques described in Voinchet et al. (2004). Aliquots were irradiated using a panoramic ^{60}Co source (Dolo et al., 1996) with 1.25 MeV gamma rays and a dose rate of 200 Gy/h. Applied irradiation dose values range from 260 to 12,000 Gy.

ESR measurements were performed on 100–200 μm quartz grains. The MNHN team measured the Al signal only in all the quartz samples, whereas the BRGM applied the MC approach on two of the four samples analysed (TVL1302 and TVL1304). The residual (non-bleachable) part of the Al signal was determined after exposing the samples to UV light in a Dr Hönhle SOL2 solar simulator for about 1600 h. The light intensity received by each artificially bleached samples was comprised between 3.2 et 3.4.10⁵ Lux. ESR measurements were performed at 107 K with an EMX Bruker ESR X-band spectrometer using the experimental conditions outlined by Voinchet et al. (2004). Al-signal intensities were measured from the top of the first peak of the hyperfine structure of the quartz ESR spectra at $g = 2.018$ and the bottom of the 16th peak at $g = 2.002$ (Toyoda and Falguères, 2003).

The Ti-Li centre intensity was measured from the bottom of the peak at $g = 1.913$ to the baseline (so called option D in Duval and Guilarte, 2015) and the Ti-H centre signal intensity from the bottom of the doublet at $g = 1.915$ to the baseline (so called option C in Duval and Guilarte, 2015). For each centre, the average and the standard deviation of three repeated measurements were calculated and used for D_e determination.

Dose response curves (DRCs) were obtained by fitting an exponential + linear equation (E + L) function through the experimental data points (Duval, 2012; Cordier et al., 2012). Fitting was performed using Microcal OriginPro 8, with data weighted by the inverse of the square intensities.

The analytical protocols used by the two teams are compared in Table 2. Sample preparation, dose rate evaluation and age calculation are strictly similar for the two procedures. Both teams used measured water content for dose rate evaluation. The main differences concern: (i) the use of the MC approach by BRGM team; (ii) the maximal dose of irradiation (D_{max}) employed by each team (9,870 Gy for MNHN vs 11,700 Gy for BRGM); (iii) the water content considered for the age calculation (5–8% for MNHN and 10–12% for BRGM, which is most likely the result of different weather conditions before and during sampling).

Table 2

Comparison of the analytical protocols used by the MNHN and BRGM teams for the ESR dating of the Tourville sediments.

Analytical protocol	MNHN	BRGM
Preparation	Quartz extraction and purification procedure following Voinchet et al. (2004)	
Selected grain size	100–200 μm	
Number of irradiation steps	10	
D_{max}	9,870 Gy	11,700 Gy
ESR signal	Al (Toyoda and Falguères, 2003)	Al (Toyoda and Falguères, 2003), Ti-Li and Ti-H (Toyoda et al., 2000; Tissoux et al., 2008)
ESR intensity	Al -From the top of the peak at $g = 2.018$ and the bottom of the 16th peak at $g = 2.002$	Ti-Li - from the bottom of the peak at $g = 1.913$ to the baseline Ti-H - from the bottom of the doublet at $g = 1.915$ to the baseline
Fitting function (data weighting)	E + L (1/I ²)	
Fitting program	Origin	
Alpha efficiency	0.15 \pm 0.10 (Laurent et al., 1998)	
Sediment radioelement contents	Determined by HRGS	
Post Rn disequilibrium in the U-238 series	No disequilibrium observed	
Water content of sediment	Measured values (5–8% wgt)	15 \pm 5% wgt (measured values:10–12% wgt)
<i>In situ</i> gamma measurements	Yes (NaI probe, Inspector 1000, Canberra), directly at the sampling spot	Yes (NaI probe, Digidart LF gamma, Ortec), directly at the sampling spot
Cosmic dose rate	Calculated from present-day depth (according to the tables of Prescott and Hutton, 1988, 1994)	
Grain size attenuation for alpha and beta dose rate	Brennan (2003) and Brennan et al. (1991)	
Dose rate factor conversions	Adamiec and Aitken (1998)	
Age calculation program	ESR MNHN program	

Table 3
U-series and ESR data obtained by the CENIEH-RSES team (modified from Faivre et al., 2014).

Sample	Tissue	U (ppm)	²³⁴ U/ ²³⁸ U	²³⁰ Th/ ²³⁸ U	Apparent U-series age (ka)	Initial enamel Thickness (μm)	Removed thickness (μm)	Depth (m)	Sediment radioelement contents			D _E (Gy)
									U (ppm)	Th (ppm)	K (%)	
T1	enamel	0.39 ± 0.00	1.2266 ± 0.0483	0.6211 ± 0.0331	75.1	1160 ± 116	(1): 100 ± 10	21 ± 3	1.11 ± 0.02	4.09 ± 0.02	0.67 ± 0.02	121 ± 2
	dentine	19.68 ± 0.12	1.2366 ± 0.0127	0.7922 ± 0.0471	106.8		(2): 110 ± 11					
T2	enamel	0.53 ± 0.02	1.2110 ± 0.0882	1.0357 ± 0.1012	189.0	1010 ± 101	(1): 110 ± 11	21 ± 3	1.11 ± 0.02	4.09 ± 0.02	0.67 ± 0.02	175 ± 2
	dentine	28.49 ± 0.97	1.3172 ± 0.0032	1.0415 ± 0.0103	154.0		(2): 100 ± 10					
T3	enamel	0.42 ± 0.11	1.2097 ± 0.0383	0.7048 ± 0.1833	92.3	1300 ± 130	(1): 90 ± 9	20 ± 3	0.88 ± 0.02	3.73 ± 0.02	0.72 ± 0.02	142 ± 4
	dentine	28.19 ± 1.64	1.2468 ± 0.0070	0.8435 ± 0.0155	116.8		(2): 120 ± 12					
T4	enamel	0.41 ± 0.14	1.2398 ± 0.0471	1.3390 ± 0.1092	656.2	900 ± 90	(1): 110 ± 11	21 ± 3	1.47 ± 0.02	3.52 ± 0.02	0.67 ± 0.02	165 ± 2
	dentine	24.10 ± 1.97	1.3209 ± 0.0102	1.0818 ± 0.0175	165.5		(2): 90 ± 9					
T5	enamel	0.71 ± 0.27	1.3082 ± 0.0475	1.2751 ± 0.0742	265.7	970 ± 97	(1): 50 ± 5	21 ± 3	1.47 ± 0.02	3.52 ± 0.02	0.67 ± 0.02	155 ± 4
	dentine	23.04 ± 0.93	1.3608 ± 0.0084	1.2050 ± 0.0585	196.1		(2): 80 ± 8					
T6	enamel	0.41 ± 0.12	1.1931 ± 0.0360	0.8108 ± 0.0746	118.8	890 ± 89	(1): 30 ± 3	21 ± 3	0.88 ± 0.02	3.73 ± 0.02	0.72 ± 0.02	153 ± 4
	dentine	27.85 ± 2.43	1.2029 ± 0.0069	0.8059 ± 0.0067	115.7		(2): 60 ± 6					
	cementum	29.98 ± 6.69	1.2836 ± 0.0059	0.8287 ± 0.0326	107.5							
T7	enamel	0.49 ± 0.18	1.2791 ± 0.0578	0.7844 ± 0.1109	99.1	1050 ± 105	(1): 20 ± 2	21 ± 3	0.88 ± 0.02	3.73 ± 0.02	0.72 ± 0.02	164 ± 4
	dentine	29.90 ± 1.15	1.2096 ± 0.0080	0.7702 ± 0.0055	106.2		(2): 60 ± 6					
	cementum	37.26 ± 1.27	1.3047 ± 0.0105	0.7773 ± 0.0124	94.5							
T8	enamel	0.82 ± 0.37	1.3203 ± 0.0437	1.1941 ± 0.1182	209.8	840 ± 84	(1): 40 ± 4	20 ± 3	0.87 ± 0.02	3.77 ± 0.02	0.72 ± 0.02	254 ± 4
	dentine	17.76 ± 0.46	1.3777 ± 0.0089	1.3479 ± 0.0132	259.6		(2): 60 ± 6					

Dental tissue	p U-uptakeparameter (a.u.)	D _{internal} (μGy/a)	D _{βdentine} (μGy/a)	D _{βsediment} (μGy/a)	D _(γ+cosm) (μGy/a)	D _a (μGy/a)	ESR-U-series age (ka)	CS-US-ESR age (ka)
T1 enamel	-0.09 ± 0.27	56 ± 16	133 ± 33	61 ± 11	405 ± 55	656 ± 67	184 + 26 - 19	201 ± 25
T1 dentine	-0.51 ± 0.20							
T2 enamel	-0.93 ± 0.06	185 ± 33	344 ± 63	68 ± 12	405 ± 52	1003 ± 88	174 + 17 - 14	188 ± 21
T2 dentine	-0.93 ± 0.06							
T3 enamel	-0.12 ± 0.50	71 ± 40	173 ± 36	55 ± 10	381 ± 48	680 ± 72	208 ± 28 - 22	236 ± 29
T3 dentine	-0.49 ± 0.14							
Weighted mean							194 + 14 - 11	211 ± 15

5. Results

5.1. Combined ESR/U-series age estimates on teeth

5.1.1. CENIEH-RSES

A summary of the analytical data and results obtained by the CENIEH-RSES team is given in in Table 3. Three of the teeth from lower D2 level (T4, T5 and T8) show the highest apparent U-series ages, which precluded any combined US-ESR age calculation for these samples. In contrast, the tooth samples from the upper D2 show a somewhat distinct pattern. The cement tissues of samples T6 and T7 have apparent U-series ages that are significantly older than the other tissues, which again precluded a straightforward US-ESR calculation. In summary, combined US-ESR age calculation was possible for only 3 of the 8 teeth (see also Faivre et al., 2014). All resulting age estimates are within the one-sigma error range. They are between ~174 ka and ~208 ka for teeth T1, T2 (both from lower D2) and T3 (from the upper part of D2). The limited age scatter (relative standard deviation of about 9%) may be partially explained by some lateral variations in the sediment radioactivity: the external dose rate derived from the different sediment

samples collected within D2 varies by about 4%.

Interestingly, the CSUS-ESR estimates are somewhat older but nevertheless consistent with the standard US-ESR ages, indicating thus that the U-uptake modelling has a very limited impact on the final age results. They vary between 188 ± 21 and 236 ± 29 ka (Table 3). Based on the weighted mean US-ESR and CSUS-ESR ages, the best age range estimate for the teeth derives from the error range given by both models, i.e. 183 to 226 ka, which represents the middle part of MIS 7 to the beginning of MIS 6.

5.1.2. MNHN

Although the combined US-ESR age results obtained by the MNHN team have been published earlier in Bahain et al. (2015), the data obtained were not fully given and will therefore be detailed in the present paper (Table 4).

Contrary to the earlier dating study by Faivre et al. (2014), the use of the US model for the age calculation was possible for all the teeth, indicating more homogeneous U-uptake behaviours and no occurrence of uranium leaching. The teeth analyzed by the MNHN team display relatively similar paleodosimetric parameters: the D_e dispersion is low

Table 4

U-series and ESR data obtained by the MNHN team. Analytical uncertainties are given with $\pm 1\sigma$. * The depth was estimated from the chronostratigraphic interpretation of [Jamet \(2015\)](#).

Sample	Dental tissue	U (ppm)	$^{234}\text{U}/^{238}\text{U}$	$^{230}\text{Th}/^{238}\text{U}$	Apparent U-series age (ka)	$^{222}\text{Rn}/^{230}\text{Th}$	Initial enamel thickness (μm)	Removed thickness (μm)	Mean depth (m) *	D_e (Gy)
TVL 157	enamel	0.594 \pm 0.024	1.441 \pm 0.069	1.222 \pm 0.101	174	0.334	959 \pm 17	(1) 21 \pm 3	14 \pm 3	220.08 \pm 2.33
	dentine	25.342 \pm 0.580	1.306 \pm 0.026	1.028 \pm 0.052	153	0.366		(2) 74 \pm 9		
TVL 160	enamel	0.402 \pm 0.016	1.313 \pm 0.060	1.155 \pm 0.102	195	1.000	1050 \pm 131	(1) 28 \pm 3	14 \pm 3	207.72 \pm 2.72
	dentine	22.504 \pm 0.486	1.333 \pm 0.026	1.152 \pm 0.049	186	0.340		(2) 160 \pm 20		
TVL 219	enamel	0.671 \pm 0.022	1.259 \pm 0.043	0.993 \pm 0.081	155	0.405	1027 \pm 128	(1) 14 \pm 2	14 \pm 3	204.54 \pm 2.49
	dentine	31.541 \pm 0.636	1.274 \pm 0.022	0.956 \pm 0.048	140	0.378		(2) 167 \pm 21		
TRV 923	enamel	0.490 \pm 0.018	1.301 \pm 0.054	1.106 \pm 0.094	181	0.259	958 \pm 120	(1) 68 \pm 9	14 \pm 3	204.56 \pm 1.09
	dentine	29.026 \pm 0.741	1.261 \pm 0.028	1.005 \pm 0.058	159	0.293		(2) 76 \pm 9		
TRV 928	enamel	0.296 \pm 0.014	1.409 \pm 0.076	1.305 \pm 0.116	217	0.258	1268 \pm 159	(1) 200 \pm 25	14 \pm 3	191.33 \pm 5.82
	dentine	19.976 \pm 0.348	1.311 \pm 0.021	1.053 \pm 0.083	159	0.523		(2) 148 \pm 18		
TVL 929(a)	enamel	0.374 \pm 0.013	1.236 \pm 0.047	0.973 \pm 0.086	155	0.247	1200 \pm 150	(1) 112 \pm 14	14 \pm 3	191.95 \pm 2.73
	dentine	3.046 \pm 0.067	1.263 \pm 0.025	0.988 \pm 0.054	153	1.000		(2) 60 \pm 8		

Sample	Sediment radioelement contents			Dental tissue	p U-uptake parameter (a.u.)	D_a ($\mu\text{Gy/a}$)	D_g ($\mu\text{Gy/a}$)	$D_{(y+\text{cosm})}$ ($\mu\text{Gy/a}$)	D_a ($\mu\text{Gy/a}$)	US-ESR age (ka)	CSUS-ESR age (ka)
	U (ppm)	Th (ppm)	K (%)								
TVL 157	1.072	4.005	0.894	enamel	-0.83 \pm 0.04	139	305	517	961	229	252
	\pm 0.086	\pm 0.114	\pm 0.014	dentine	-0.72 \pm 0.05	\pm 27	\pm 42	\pm 29	\pm 58	\pm 13	\pm 16
TVL 160	1.252	4.341	0.902	enamel	-0.91 \pm 0.03	100	294	517	911	228	239
	\pm 0.074	\pm 0.099	\pm 0.011	dentine	-0.88 \pm 0.03	\pm 19	\pm 44	\pm 29	\pm 56	\pm 13	\pm 12
TVL 219	1.293	3.807	0.853	enamel	-0.82 \pm 0.05	142	349	517	1008	203	223
	\pm 0.076	\pm 0.102	\pm 0.012	dentine	-0.73 \pm 0.05	\pm 28	\pm 55	\pm 29	\pm 61	\pm 13	\pm 14
TRV 923	1.065	3.716	0.837	enamel	-0.88 \pm 0.04	103	314	517	934	219	232
	\pm 0.063	\pm 0.084	\pm 0.010	dentine	-0.78 \pm 0.04	\pm 21	\pm 47	\pm 29	\pm 59	\pm 13	\pm 14
TRV 928	1.120	3.735	0.799	enamel	-0.93 \pm 0.03	75	176	517	768	249	268
	\pm 0.078	\pm 0.103	\pm 0.012	dentine	-0.69 \pm 0.05	\pm 26	\pm 39	\pm 29	\pm 55	\pm 15	\pm 15
TVL 929(a)	1.151	3.678	0.807	enamel	-0.74 \pm 0.04	65	271	517	853	225	240
	\pm 0.086	\pm 0.114	\pm 0.014	dentine	-0.73 \pm 0.05	\pm 14	\pm 43	\pm 29	\pm 54	\pm 13	\pm 13
Weighed mean										224 \pm 11	241 \pm 11

(from 191 \pm 6 to 220 \pm 2 Gy, around 6%; [Table 4](#)); the p parameters describe early uptake (p values between -0.93 and -0.69, [Table 4](#)) for all the tissues; the external environmental dose rate measured *in situ* within the D2 layer shows a very limited lateral variability (5%), demonstrating thus the homogeneity of the sedimentary environment (a mean value of 417 \pm 21 $\mu\text{Gy/a}$ was used for the age calculation). Hence, the age results obtained for the six teeth show relatively little scatter, i.e. between 203 \pm 13 ka and 249 \pm 15 ka. A mean age of 224 \pm 11 ka could be calculated using IsoPlot 3.0 software ([Ludwig, 2003](#)) for the D2 level, unequivocally placing the deposition of this layer during MIS7, and probably during the first part of this stage. A consistent CSUS-ESR weighted mean age of 241 \pm 11 ka was obtained, indicating that the U-uptake modelling has a very limited impact on the final age result, similarly to the other dating results obtained by [Favre et al. \(2014\)](#).

5.2. ESR on optically bleached quartz grains

5.2.1. MNHN

The radioelement contents, ESR ages and associated dose rate contributions determined for the Tourville-la-Rivière D1 and D2 sediments at MNHN are displayed in [Table 5](#).

Even if bleaching coefficients vary within narrow range for the whole set of samples from D2 (from 42 to 51%; [Table 5](#)), the equivalent dose values differ by a factor of 2.6, while the dose rate are all around 1100–1200 $\mu\text{Gy/a}$. Consequently, the resulting ESR ages significantly vary, from 349 \pm 30 to 906 \pm 70 ka. In comparison, the two ESR ages obtained for the D1 level show a limited scatter, with values ranging from 334 \pm 90 to 390 \pm 60 ka. This difference between the two levels is probably related with the deposition environment: D1 level is made of coarser sediments than D2, indicating a deposition along the river bank rather than in the floodplain in high water periods. This may

explain why bleaching appears to be more homogeneous among D1 samples compared with D2. Following the principles of the MC approach, all these ESR age results obtained from the measurement of the Al centre only should in first instance be interpreted as maximum possible burial age estimates for D1 and D2 levels.

5.2.2. BRGM

The results obtained for the samples processed by the BRGM team are displayed in [Table 6](#). The MC approach was employed for two samples (TVL-1302 and TVL-1304) while only the Al-signal was measured for the two other samples.

In the D1 level, bleaching coefficients of the Al centre determined by the BRGM team are close to those obtained by the MNHN one (42 vs. 46%). Similarly, the total dose rate values are slightly lower but nevertheless consistent at a one-sigma level. In particular, the *in situ* gamma dose rate of TVL-1304 is the same as the dose measured by MNHN team in this level (samples Tourville 5 and 6; [Table 5](#)). Interestingly, both Al and Ti-Li ESR ages are in close agreement around 980–990 ka, and both significantly older than the results derived from MNHN samples of the same level (334 \pm 90 & 390 \pm 60 ka; [Table 4](#)). In contrast, Ti-H signal provides a significantly younger age of 243 \pm 14 ka. Following the principles of the MC approach, these age differences between Al, Ti-Li and Ti-H centres may simply reflect an incomplete bleaching of the former two signals during sediment transport. Consequently, the Ti-H age result is interpreted as being the closest estimate to the true burial age of the sample. This age is actually highly consistent with those derived from the teeth of level D2 above ([Tables 3 and 4](#)).

In contrast, the three samples from level I display very close total dose rate values (around 500–550 $\mu\text{Gy/a}$) and highly scattered D_e estimates from the Al centre ranging from 187 \pm 73 Gy to 737 \pm 178 Gy. As a consequence, The Al ESR ages vary from

Table 5

Radioelement contents, equivalent doses, bleaching rate, dose rate contributions and ESR ages obtained for the sediments of the Tourville-la-Rivière D1 and D2 levels dated by the MNHN team. The bleaching coefficient represents the relative difference between the ESR intensities of the natural and bleached aliquots. Analytical uncertainties are given with $\pm 1\sigma$.

Sample	Level	U (ppm)	Th (ppm)	K (%)	Al Bleaching coefficient (%)	D_e (Gy)	D_α ($\mu\text{Gy/a}$)	D_β ($\mu\text{Gy/a}$)	<i>in situ</i> D_γ ($\mu\text{Gy/a}$)	D_{cosmic} ($\mu\text{Gy/a}$)	D_a ($\mu\text{Gy/a}$)	Age (ka)
Tourville 1	D2	1.014 \pm 0.074	3.270 \pm 0.103	0.748 \pm 0.012	44	409 \pm 56	26 \pm 1	622 \pm 17	393 \pm 20	102 \pm 5	1144 \pm 22	358 \pm 50
Tourville 2	D2	0.895 \pm 0.083	3.133 \pm 0.114	0.728 \pm 0.014	42	398 \pm 30	24 \pm 1	595 \pm 19	418 \pm 20	102 \pm 5	1139 \pm 50	349 \pm 30
Tourville 3	D2	0.993 \pm 0.086	3.460 \pm 0.118	0.756 \pm 0.014	49	708 \pm 87	27 \pm 1	629 \pm 20	412 \pm 20	102 \pm 5	1170 \pm 26	605 \pm 80
Tourville 4	D2	0.990 \pm 0.072	3.567 \pm 0.099	0.741 \pm 0.012	51	1085 \pm 76	27 \pm 1	621 \pm 17	447 \pm 20	102 \pm 5	1198 \pm 21	906 \pm 70
Tourville 5	D1	0.767 \pm 0.046	1.677 \pm 0.057	0.426 \pm 0.006	46	246 \pm 32	16 \pm 1	370 \pm 10	260 \pm 13	89 \pm 4	736 \pm 13	334 \pm 90
Tourville 6	D1	0.711 \pm 0.067	1.978 \pm 0.080	0.447 \pm 0.010	46	295 \pm 40	18 \pm 1	389 \pm 15	260 \pm 13	89 \pm 4	756 \pm 19	390 \pm 60

535 \pm 22 to 1354 \pm 283 ka. The Ti-Li signal measured in sample TVL-1302 displays a significantly younger age estimate (by about 44%) compared with that of the Al signal. Similarly, the Ti-H signal produced an even younger result (-27% compared with Ti-Li). This pattern is comparable to that observed for TVL-1304: it suggests an incomplete reset of both the Al and Ti-Li signals prior to sediment burial. In accordance with the MC approach, the Ti-H signal most likely provides the closest estimate (236 \pm 49 ka) to the true burial age for this sample.

Samples TVL-1304 (level D1) and TVL-1302 (level I) are located at the bottom and top of the local sequence, respectively, and bracket the human occupation from level D2. They provide very close Ti-H ESR age results (243 \pm 14 vs. 236 \pm 49 ka). As consequence, no apparent stratigraphic pattern is observed. This may be interpreted in first instance as an evidence of relatively rapid sedimentation from D1 to I levels. These results allow the correlation of these levels to MIS7.

6. Discussion

The two sets of ESR and U-series data obtained on fossil teeth by the two independent teams involved in the Tourville study are overall in good agreement (Fig. 5). However, the CENIEH-RSES samples displays more scattered D_e (Fig. 5A) and U-series (Fig. 5B) data than MNHN, while uranium concentration values in dental tissues overall vary within the same range (Fig. 5C).

We can observe in particular that a majority of the CENIEH-RSES teeth recovered during the 2010 excavation are close or beyond of the

U-series applicability domain, preventing the use of US model for these teeth (Fig. 5B). The overall smaller D_e values obtained for most of the teeth (Fig. 5A) also constitute an additional limiting factor, which explains why US-ESR ages could only be calculated for three teeth. In comparison, the MNHN teeth recovered during the 2008 excavation provide more homogeneous ESR and U-series data and seem to have experienced relatively simple (and relatively early) U-uptake histories, with p-values ranging between -1 and -0.7 . In contrast, CENIEH-RSES have apparently experienced more complex U-uptake, including U-leaching. This difference could be correlated to the origin of the teeth, with one excavation area (2008) that underwent more favorable geochemical conditions from an ESR dating perspective in comparison with the other (2010 area). This hypothesis is supported by the fact that two of the three CENIEH-RSES teeth that could be dated are spatially located the closest to the 2008 excavation area (Fig. 3).

The MNHN tooth samples yield a weighted mean US-ESR and CSUS-ESR age of 224 \pm 11 ka and 241 \pm 11 ka, respectively. CENIEH-RSES results are both $\sim 14\%$ lower with 194 $^{+14}_{-11}$ ka and 211 \pm 15 ka for the US and CSUS models, respectively. Nevertheless, both data sets overall at a two-sigma confidence level, supporting thus their consistency. Consequently, US-ESR and CS-US-ESR weighted mean ages of 218 \pm 16 ka and 236 \pm 16 ka may be calculated, respectively (Fig. 5D). These results permit to unambiguously correlate the human occupation of the D2 level to MIS 7.

Although both independent data sets are consistent, we acknowledge that there may be a systematic component in the uncertainty due to differences in the analytical procedures, which might partly explain

Table 6

Radioelement contents, equivalent doses, bleaching rate, dose rates contributions and ESR ages obtained for the sediments of the Tourville-la-Rivière D1 and I levels analyzed by the BRGM team. Analytical uncertainties are given with $\pm 1\sigma$.

Sample	Level	U (ppm)	Th (ppm)	K (%)	ESR Centre	Bleaching rate (%)	D_e (Gy)	D_α ($\mu\text{Gy/a}$)	D_β ($\mu\text{Gy/a}$)	<i>in situ</i> D_γ ($\mu\text{Gy/a}$)	D_{cosmic} ($\mu\text{Gy/a}$)	D_a ($\mu\text{Gy/a}$)	Age (ka)
TVL1301	I	0.320 \pm 0.038	0.822 \pm 0.043	0.361 \pm 0.005	Al	37	335 \pm 62	9 \pm 1	307 \pm 9	176 \pm 55	47 \pm 2	538 \pm 56	565 \pm 32
TVL1302	I	0.356 \pm 0.042	0.830 \pm 0.048	0.347 \pm 0.006	Al	43	332 \pm 113	9 \pm 1	302 \pm 10	163 \pm 55	47 \pm 2	521 \pm 56	577 \pm 120
					Ti-Li	100	187 \pm 73						325 \pm 68
					Ti-H	100	136 \pm 39						236 \pm 49
TVL1303	I	0.262 \pm 0.039	0.713 \pm 0.044	0.333 \pm 0.005	Al	41	737 \pm 178	7 \pm 1	278 \pm 9	172 \pm 60	47 \pm 2	504 \pm 61	1354 \pm 283
TVL1304	D1	0.573 \pm 0.043	1.377 \pm 0.051	0.400 \pm 0.006	Al	42	687 \pm 255	14 \pm 1	362 \pm 10	260 \pm 54	38 \pm 2	674 \pm 55	981 \pm 204
					Ti-Li	100	696 \pm 183						994 \pm 206
					Ti-H	100	170 \pm 13						243 \pm 14

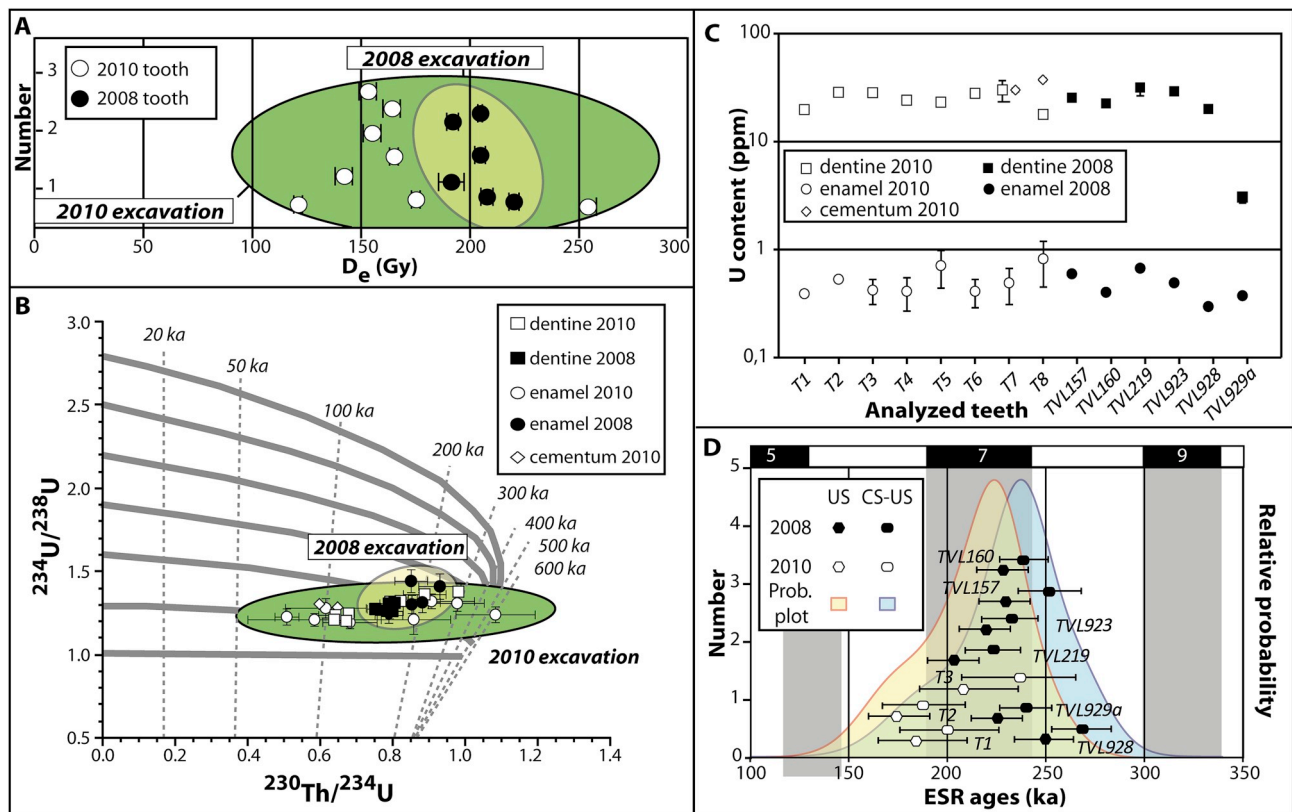


Fig. 5. ESR/U-series data obtained on the Tourville-la Rivière teeth analyzed by the CENIEH-RSES and MNHN teams. A) Equivalent dose values; B) U-series data; C) U-content of the dental tissues; D) ESR/U-series (US and CS-US) and corresponding age density probability plots.

Table 7
Comparison of the equivalent dose values obtained with or without use of Duval and Grün (2016)'s recommendations.

Sample	CENIEH-RSES (Faivre et al., 2014)			This study			Ratio
	D _{e-1} (Gy)	D _{max} (Gy)	D _{max} /D _{e-1}	D _{e-2} (Gy)	D _{max} (Gy)	D _{max} /D _{e-2}	
T1	121 ± 2	5,000	41	121 ± 3	1,000	8	1.00
T2	175 ± 2	5,000	29	178 ± 4	1,000	6	1.02
T3	142 ± 4	5,000	35	134 ± 4	1,000	7	0.94
T4	165 ± 2	5,000	30	160 ± 2	1,000	6	0.97
T5	155 ± 4	5,000	32	150 ± 7	1,000	7	0.97
T6	153 ± 4	5,000	33	149 ± 7	1,000	7	0.97
T7	164 ± 4	5,000	30	151 ± 5	1,000	7	0.92
T8	254 ± 4	5,000	20	251 ± 8	1,800	7	0.99
Mean ± s.d.	166 ± 28 (17%)			153 ± 22 (14%)			0.97

Sample	MNHN (Bahain et al., 2015)			This study			Ratio
	D _{e-1} (Gy)	D _{max} (Gy)	D _{max} /D _{e-1}	D _{e-2} (Gy)	D _{max} (Gy)	D _{max} /D _{e-2}	
TVL157	221 ± 3	5,000	23	217 ± 7	1,249	6	0.98
TVL160	208 ± 3	5,000	24	206 ± 6	1,249	6	0.99
TVL219c	205 ± 2	5,000	24	193 ± 5	1,249	6	0.94
TVL923	205 ± 1	5,000	24	201 ± 3	1,249	6	0.98
TVL928	191 ± 6	5,000	23	169 ± 6	1,249	7	0.88
TVL929	191 ± 6	5,000	26	183 ± 4	1,249	7	0.96
Mean ± s.d.	207 ± 6 (3%)			195 ± 14 (7%)			0.96

this overall 14% age underestimation of the CENIEH-RSES vs MNHN age results. This age underestimation may be the result of either a D_e underestimation or a dose rate overestimation, or possibly a combination of both.

For example, the impact of the absence of *in situ* gamma dose rate evaluation for the CENIEH-RSES samples can hardly be evaluated. If the impact of the water contents used for age calculations is low (less than 2%) for both dental tissues and sediment, it could be envisaged in first instance that a somewhat overestimated gamma dose rate has been

derived from the laboratory analysis of unrepresentative (at a gamma-ray scale) sediment samples. However, the gamma + cosmic dose rate estimated for 2/3 CENIEH-RSES samples are already significantly lower than those obtained for the MNHN samples, mainly in relation to the cosmic dose rate used for the age calculation (26.8 μGy/a for the CENIEH-RSES samples vs 100 μGy/a for the MNHN ones). Consequently, an additional overestimation of this parameter may be considered as unlikely.

The impact of using different dose rate conversion factors (Adamic

and Aitken (1998) and Guérin et al. (2011) for MNHN and CENIEH-RSES, respectively) is typically estimated to be < 1% (e.g., Liritzis et al., 2013), and can therefore here considered to be negligible. Finally, any bias induced by the use of different combined ESR/U-series age calculation programs is also to be negligible (< 1%), as shown earlier in the comparison study by Shao et al. (2014).

Additionally, the D_e values initially considered by Faivre et al. (2014) and Bahain et al. (2015) have been recalculated based on the more recent work by Duval and Grün (2016) for the selection of the maximum applied dose (D_{max}) in order to avoid D_e overestimation. Based on their recommendations, and given the magnitude of the D_e values (between 100 and 250 Gy), the D_{max}/D_e ratio should be somewhere of between 5 and 10, whereas it is ranging from 20 to 41 for the previously published data (see Table 7). Consequently, new fittings were performed with the same program (Origin), function (SSE), data weighing option ($1/I^2$) and the appropriate D_{max}/D_e ratio. The resulting D_e values remain all within error, although a slight mean decrease of about 3% of about 6% may be observed for the CENIEH-RSES and MNHN data sets, respectively. One may note that the errors on the revised D_e values are overall higher than those obtained earlier, which is simply the result of a fitting performed with a more reduced number of experimental data points (6–8 instead of 10 previously). In summary, the use of a smaller D_{max} value has a very limited impact on the corrected D_e value for most of the teeth, and is most likely not the main reason for the overall age difference of ~14% between the two data sets.

In fact, most of this age difference probably comes from the consideration of radon loss from dental tissues by the MNHN team, while a radioactive equilibrium was assumed by the CENIEH-RSES team. The Rn loss measured on both dentine and enamel of the MNHN teeth is quite important for the most of the analyzed tissues ($^{222}\text{Rn}/^{230}\text{Th}$ ratio ranging from 0.247 to 0.523, except for two tissues showing equilibrium, Table 4). If equilibrium was assumed for these tissues, this would lead to a decrease of the age estimates ranging from –20.7 to –5.8% depending on the samples considered. Moreover, it would no longer be possible to use the US model for two samples (TVL 160 and TVL 923).

Lastly, if the MNHN ages are recalculated using the CENIEH-RSES parameters (conversion factors from Guérin et al. (2011) same water contents of dental tissues and sediments, Rn equilibrium, cosmic dose corresponding to a 21 m-depth, gamma dose calculated from the sediment contents), the age estimates decrease for four samples (–12.0 to –13.8%) and increase for two of them (+1.2 to +8.0%) leading to a reduced mean age difference of –7.8% between the two sets of samples.

Concerning ESR dating of quartz, all the Al and Ti-Li ESR ages look strongly overestimated (in perhaps a lesser extent for the Ti-Li) compared with the existing chronological framework, the combined ESR/U-series ages and Ti-H ESR ages (Fig. 6). In accordance with the principles of the MC approach, this overestimation is most likely due to incomplete bleaching (Duval et al., 2017). The geological nature of the D2 sediment (silty clayey deposits) could indicate a turbid water deposit in a decantation environment such as floodplain or muddy supratidal area. It could explain the age overestimate for Al and Ti-Li centres in this level (see also Voinchet et al., 2015). A similar hypothesis can be made for sandy levels D1 and I. The fluvio-estuarine origin of the sediments seems to constitute an unfavorable environment to completely reset the Al and Ti-Li signals.

In comparison, given its bleaching kinetics, Ti-H centre is by definition most likely to have been fully reset during sediment transport. Ti-H ESR results (243 ± 14 ka and 236 ± 49 ka for units D1 and I respectively) in close agreement with the US-ESR ages obtained on fossil teeth (weighted mean age of 218 ± 16 ka). All together, these data consistently date the deposition of the Tourville D1 to I units to the first part of MIS 7 rather than to the end of this interglacial stage as previously considered (Lautridou, 1985; Balescu et al., 1997). These results

demonstrate the importance of using the MC approach in ESR dating of optically bleached quartz grains, which is the only way to evaluate potential incomplete bleaching of Al and Ti centres prior to burial.

7. Conclusion

Tourville-la-Rivière is one of the very few Middle Pleistocene localities where successive and independent ESR and ESR/U-series dating studies have been performed by different teams. The ESR and U-series analyses of fossil teeth show two different populations of samples with different characteristics: the MNHN samples from the 2008 excavation are displayed homogeneous ESR and U-series data and seem to have experienced relatively simple U-uptake histories, while the scattered results obtained on CENIEH-RSES teeth (2010 excavation area) indicate a more complex evolution, including uranium leaching processes. Despite some differences in the analytical protocols independently used by each team, combined ESR/U-series age results consistently position the palaeontological remains and lithic series of D2 layer within MIS7.

Concerning the ESR dating of optically bleached quartz grains, the two studies performed by the MNHN and BRGM teams show clearly that the sedimentary environments from the clayey unit D2, and the sandy units D1 and I, were simply not suitable to completely reset the ESR signals of the Al and Ti-Li centres. In contrast, the Ti-H centre provides age estimates that are in agreement with the ESR/U-series results. This demonstrates the great potential of this centre to date late Middle Pleistocene deposits, which is consistent with previous observations by Duval et al. (2017). A multiple centre approach seems therefore indispensable when dating this type of fluvio-estuarine sediment, even when the sedimentological characteristics of the sediments seem initially quite suitable for an ESR study (as it was the case for the Tourville D1 and I units). Similar observations have been recently made on fluvial deposits from Spain (Duval et al., 2017; Méndez-Quintas et al., 2018), Italy (Pereira et al., 2015, 2018; Voinchet et al., this issue) or France (Duval et al., submitted).

Despite some (expected) discrepancies related to the independent use of parameters and approaches by the different teams involved in this multi-laboratory study, the whole set of ESR and ESR/U-series data collected at Tourville-la-Rivière locality consistently correlates stratigraphic levels D1 to I and associated human occupation to MIS7.

Acknowledgments

For the CENIEH-RSES team, the ESR/U-series study was initially funded by the project GGL 2010-16821 from the Spanish Ministry of Science and Innovation and the Australian Research Council DP110101415. Aspects of this research have been covered by the ARC Future Fellowship Grant FT150100215. The authors thank Carlos Saiz and Verónica Guilarte, CENIEH, for their helpful contribution during sample preparation and ESR measurements. They thank also the two anonymous referees for their comments and suggestions that have greatly improved the manuscript.

The Muséum national d'Histoire naturelle (MNHN) study is part of an Agence Nationale pour la Recherche project (ANR n°2010-BLANC-200601 coordinated by M.H. Moncel and D. Schreve). The MNHN team thanks Sylvie Coutard and Patrick Auguste for helpful discussion and the French Ministry of Culture for the financial support of PCR “les premiers hommes en Normandie” (coordinated by D. Cliquet). The ESR and mobile gamma-ray spectrometers of the French National Museum of Natural History were bought with the financial support of the ‘Sesame Île-de-France’ program and the ‘Région Centre’ respectively.

The Bureau de Recherche Géologique et Minière (BRGM) analyses were performed within a research project REGOMETH (PDR13DGR33). We thank also Mr Rozier, Denis and Lévêque (CBN) for the authorization of access to the Tourville Quarry.

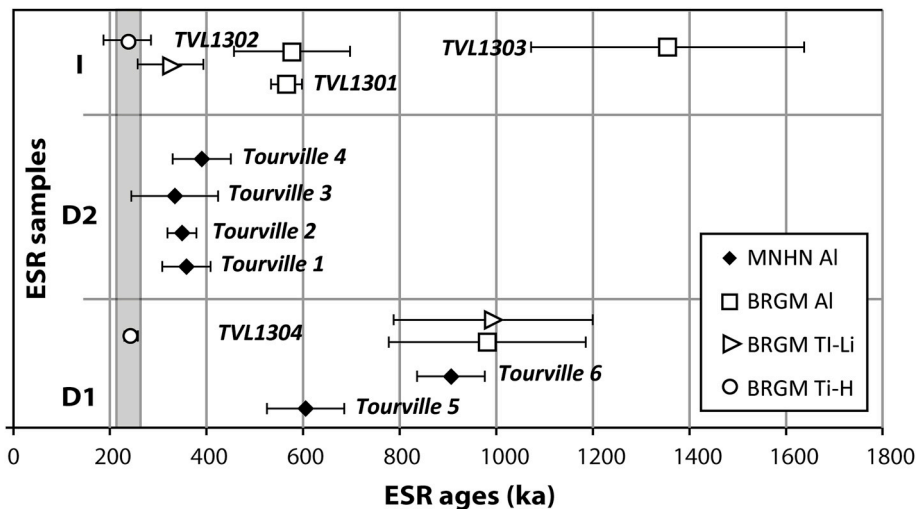


Fig. 6. ESR ages obtained on the Tourville-la Rivière sediments analyzed by the MNHN and BRGM teams using different ESR centres. The grey band corresponds to the MIS 7 time range.

Appendix A. Supplementary data

Supplementary data to this article can be found online at <https://doi.org/10.1016/j.quaint.2019.06.015>.

References

- Adamiec, G., Aitken, M., 1998. Dose-rate conversion factor: update. *Anc. TL* 16, 37–50.
- Auguste, P., 2009. Evolution des peuplements mammaliens en Europe du nord-ouest durant le Pléistocène moyen et supérieur. Le cas de la France septentrionale. *Quaternaire* 20, 527–550.
- Bahain, J.-J., Falguères, C., Shao, Q., Tombret, O., Duval, M., Dolo, J.-M., 2015. La datation ESR/U-Th de restes paléontologiques, un outil pour estimer le degré de remaniement des niveaux archéologiques ? *Quaternaire* 26, 213–223.
- Bahain, J.-J., Falguères, C., Laurent, M., Shao, Q., Dolo, J.-M., Garcia, T., Douville, E., Frank, N., Monnier, J.-L., Hallegouët, B., Laforge, M., Huet, B., Auguste, P., Liouville, M., Serre, F., Gagnepain, J., 2012. ESR and ESR/U-series dating study of several middle palaeolithic sites of Pléneuf-Val-André (Brittany, France): piègu, Les Vallées and Nantois. *Quat. Geochronol.* 10, 424–429.
- Bahain, J.-J., Yokoyama, Y., Falguères, C., Sarcia, M.N., 1992. ESR dating of tooth enamel: a comparison with K-Ar dating. *Quat. Sci. Rev.* 11, 245–250.
- Balescu, S., Lamothe, M., Lautridou, J.-P., 1997. Luminescence evidence for two Middle Pleistocene interglacial events at Tourville, northwestern France. *Boreas* 26, 61–72.
- Beerten, K., Stesmans, A., 2006. The use of Ti centers for estimating burial doses of single quartz grains: a case study from an aeolian deposit -2Ma old. *Radiat. Meas.* 41 (4), 418–424.
- Bemilli, C., 2010. Les restes fauniques : présentation du corpus et méthodologie. In: Cliquet, D. (Ed.), 2010 - Tourville-la-Rivière, Seine-Maritime. Carrières et ballastières de Normandie : La Fosse-Marmitaine. Section BD n° 24 à 30 et 32. INRAP Grand-Ouest, Caen, pp. 105 p (unpublished).
- Bemilli, C., 2014. Les restes fauniques : présentation du corpus et méthodologie. In: Faivre, J.-Ph (Ed.), 2014 - Tourville-la-Rivière, La Fosse-Marmitaine : une fenêtre sur la vallée de la Seine au cours du Pléistocène moyen récent, INRAP Grand-Ouest, Grand-Quevilly, pp. 357 p (unpublished).
- Brennan, B.J., 2003. Beta doses to spherical grains. *Radiat. Meas.* 37, 299–303.
- Brennan, B.J., Lyons, R., Phillips, S., 1991. Attenuation of alpha particle track dose for spherical grains. *Nucl. Tracks Radiat. Meas.* 18, 249–253.
- Brennan, B.J., Rink, W.J., McGuirl, E.L., Schwarcz, H.P., Prestwich, W.V., 1997. Beta doses in tooth enamel by “One Group” theory and the Rosy ESR dating software. *Radiat. Meas.* 27, 307–314.
- Chauhan, P.R., Bridgland, D.R., Moncel, M.-H., Antoine, P., Bahain, J.-J., Briant, R., Cunha, P., Despriée, J., Limondin-Lozouet, N., Locht, J.-L., Martins, A., Schreve, D.C., Shaw, A.D., Voinchet, P., Westaway, R., White, M.J., White, T.S., 2017. Fluvial deposits as an archive of early human activity: progress during the 20 years of the Fluvial Archives Group. *Quat. Sci. Rev.* 166, 114–149.
- Cliquet, D., 2010. (dir). Tourville-la-Rivière, Seine-Maritime. Carrières et ballastières de Normandie : La Fosse-Marmitaine. Section BD n° 24 à 30 et 32. INRAP Grand-Ouest, Caen, pp. 105 p (unpublished).
- Cordier, S., Harmand, D., Lauer, T., Voinchet, P., Bahain, J.-J., Frechen, M., 2012. Geochronological reconstruction of the Pleistocene evolution of the Sarre valley (France and Germany) using OSL and ESR dating techniques. *Geomorphology* 165 (166), 91–106.
- Dolo, J.-M., Lecerf, N., Mihajlovic, V., Falguères, C., Bahain, J.-J., 1996. Contribution of ESR dosimetry for irradiation of geological and archaeological samples with a 60-Co panoramic source. *Appl. Radiat. Isot.* 47, 1419–1421.
- Dirks, P.H.G.M., Roberts, E.M., Hilbert-Wolf, H., Kramers, J.D., Hawks, J., Dosseto, A., Duval, M., Elliott, M., Evans, M., Grün, R., Hellstrom, J., Herries, A.I.R., Joannes-Boyau, R., Makhubela, T.V., Placzek, C.J., Robbins, J., Spandler, C., Wiersma, J., Woodhead, J., Berger, L.R., 2017. The age of Homo naledi and associated sediments in the Rising Star Cave, South Africa. *eLife* 6, e24231.
- Duval, M., 2012. Dose response curve of the ESR signal of the Aluminum centre in quartz grains extracted from sediment. *Anc. TL* 30 (2), 1–9.
- Duval, M., 2015. Electron spin resonance (ESR) dating of fossil tooth enamel. In: Rink, W.J., Thompson, J.W. (Eds.), *Encyclopedia of Scientific Dating Methods*. Springer Netherlands, pp. 239–246.
- Duval, M., Arnold, L.J., Guilarte, V., Demuro, M., Santonja, M., Pérez-González, A., 2017. Electron spin resonance dating of optically bleached quartz grains from the Middle Palaeolithic site of Cuesta de la Bajada (Spain) using the multiple centres approach. *Quat. Geochronol.* 37, 82–96.
- Duval, M., Grün, R., 2016. Are published ESR dose assessments on fossil tooth enamel reliable? *Quaternary Geochronology* 31, 19–27.
- Duval, M., Grün, R., Parés, J.M., Martín-Francés, L., Campaña, I., Rosell, J., Shao, Q., Arsuaga, J.L., Carbonell, E., Bermúdez de Castro, J.M., 2018. The first direct ESR analysis of a hominin tooth from Atapuerca Gran Dolina TD-6 (Spain) supports the antiquity of Homo antecessor. *Quat. Geochronol.* 47, 120–137.
- Duval, M., Guilarte, V., 2015. ESR dosimetry of optically bleached quartz grains extracted from Plio-quaternary sediment: evaluating some key aspects of the ESR signal associated to the Ti-centre. *Radiat. Meas.* 78, 28–41.
- Duval, M., Voinchet, P., Arnold, L.J., Parés, J.M., Minnella, W., Guilarte, V., Demuro, M., Falguères, C., Bahain, J.-J. & Despriée, J. (submitted). A multi-technique dating study sheds new light on the chronology of two Lower Palaeolithic sites of the Middle Loire Basin, France: lunery-la Terre-des-Sablons and Brinay-la Noira. Submitted to *Quat. Int. nat.*
- Faivre, J.-P., Maureille, B., Bayle, P., Crevecoeur, I., Duval, M., Grün, R., Bemilli, C., Bonilauri, S., Coutard, S., Bessou, M., Limondin-Lozouet, N., Cottard, A., Deshayes, T., Douillard, A., Henaff, X., Pautret-Homerville, C., Kinsley, L., Trinkaus, E., 2014. Middle Pleistocene human remains from Tourville-la-Rivière (Normandy, France) and their archaeological context. *PLoS One* 9 (10), e104111.
- Falguères, C., Bahain, J.-J., Saleki, H., 1997. U-series and ESR dating of teeth from acheulian and mousterian levels at La Micoque (dordogne, France). *J. Archaeol. Sci.* 24, 537–545.
- Falguères, C., Bahain, J.-J., Yokoyama, Y., Arsuaga, J.L., Bermudez De Castro, J.M., Carbonell, E., Bischoff, J.L., Dolo, J.M., 1999. Earliest humans in Europe: the age of TD6 gran Dolina, Atapuerca, Spain. *J. Hum. Evol.* 37, 343–352.
- Forman, S.L., Pierson, J., Lepper, K., 2000. *Luminescence Geochronology. Quaternary Geochronology: Methods and Applications*. In: Sowers, J., Noller, J., WR, L. (Eds.), American Geophysical Union, Washington, DC, pp. 157–176.
- Grün, R., Katzenberger-Apel, O., 1994. An alpha irradiator for ESR dating. *Anc. TL* 12, 35–38.
- Grün, R., 2000a. An alternative for model for open system U-series/ESR age calculations: (closed system U-series)-ESR, CSUS-ESR. *Anc. TL* 18, 1–4.
- Grün, R., 2000b. Methods of dose determination using ESR spectra of tooth enamel. *Radiat. Meas.* 32 (5–6), 767–772.
- Grün, R., 2009. The DATA program for the calculation of ESR age estimates on tooth enamel. *Quat. Geochronol.* 4, 231–232.
- Grün, R., Schwarcz, H.P., Chadam, J.M., 1988. ESR dating of tooth enamel: coupled correction for U-uptake and U-series disequilibrium. *Nucl. Tracks Radiat. Meas.* 14, 237–241.
- Grün, R., Eggins, S., Kinsley, L., Moseley, H., Sambridge, M., 2014. Laser ablation U-series analysis of fossil bones and teeth. *Palaeogeogr. Palaeoclimatol. Palaeoecol.* 416, 150–167.
- Guérin, G., Mercier, N., Adamiec, G., 2011. Dose-rate conversion factors: update. *Anc. TL*

- 29, 5–8.
- Jamet, G., 2015. Réponses sédimentaires d'un bassin versant côtier aux variations glacio-eustatiques et au soulèvement plio-quaternaire : l'exemple du bassin versant côtier de la baie de Seine (Seine, Touques et Dives). PhD thesis. University of Caen, pp. 418p (unpublished).
- Kreutzer, S., Duval, M., Bartz, M., Bertran, P., Bosq, M., Eynaud, F., Verdin, F., Mercier, N., 2018. Deciphering long-term coastal dynamics using IR-RF and ESR dating: a case study from Médoc, south-west France. *Quat. Geochronol.* 48, 108–120.
- Laurent, M., Falguères, C., Bahain, J.J., Rousseau, L., Van Vliet-Lanoë, B., 1998. ESR dating of quartz extracted from Quaternary and Neogene sediments: method, potential and actual limits. *Quaternary Science Reviews* 17, 1057–1061.
- Lautridou, J.-P., 1985. Le cycle périglaciaire pléistocène en Europe du Nord-Ouest et plus particulièrement en Normandie. State doctorate thesis. Centre de Géomorphologie du CNRS éd., Caen, pp. 907.
- Liritzis, I., Stamoulis, K., Papachristodoulou, C., Ioannides, K., 2013. A re-evaluation of radiation dose-rate conversion factors. *Mediterr. Archaeol. Archaeometry* 13 (3), 1–15.
- Ludwig, K.R., 2003. Isoplot 3.0, a geochronological toolkit for microsoft excel. 4. Berkeley Geochronology Centre Special Publication, pp. 71p.
- Marsh, R.E., 1999. Beta-gradient Isochrons Using Electron Paramagnetic Resonance: towards a New Dating Method in Archaeology. MSc thesis, McMaster University, Hamilton.
- Méndez-Quintas, E., Santonja, M., Pérez-González, A., Duval, M., Demuro, M., Arnold, L.J., 2018. First evidence of an extensive Acheulean large cutting tool accumulation in Europe from Porto Maior (Galicia, Spain). *Sci. Rep.* 8, 3082.
- Mercier, N., Falguères, C., 2007. Field gamma dose-rate measurement with a NaI(Tl) detector: re-evaluation of the "threshold" technique. *Anc. TL* 25 (1).
- Occhiotti, S., Pichet, P., Rheault, L., 1987. Résultats préliminaires d'aminochronologie moyenne et basse vallée de la Seine. In: Lautridou, J.-P. (Ed.), *La Normandie, Guide d'excursion de l'Association Française pour l'Étude du Quaternaire*, additif, pp. 19.
- Pereira, A., Nomade, S., Moncel, M.-H., Voinchet, P., Bahain, J.-J., Biddittu, I., Falguères, C., Giaccio, B., Manzi, G., Parenti, F., Scardia, G., Scao, V., Sottili, G., Vietti, A., 2018. Geochronological evidences of a MIS 11 to MIS 10 age for several key Acheulian sites from the Frosinone province (Latium, Italy): archaeological implications. *Quat. Sci. Rev.* 187, 112–129.
- Pereira, A., Nomade, S., Voinchet, P., Bahain, J.-J., Falguères, C., Garon, H., Lefèvre, D., Raynal, J.-P., Scao, V., Piperno, M., 2015. The earliest securely dated hominid fossil in Italy and evidences of Acheulian human occupations during glacial MIS 16 at Notarchirico (Venosa, Basilicata, Italy). *J. Quat. Sci.* 30 (7), 639–650.
- Prescott, J.R., Hutton, J.T., 1994. Cosmic ray contributions to dose rates for Luminescence and ESR Dating: large depths and long-term time. *Radiat. Meas.* 23, 497–500.
- Prescott, J.R., Hutton, J.T., 1988. Cosmic ray and gamma ray dosimetry for TL and ESR. *Nucl. Tracks Radiat. Meas.* 14, 223–227.
- Rixhon, G., Briant, R.M., Cordier, S., Duval, M., Jones, A., Scholz, D., 2017. Revealing the pace of river landscape evolution during the Quaternary: recent developments in numerical dating methods. *Quaternary Science Reviews* 166, 91–113.
- Sahnouni, M., Parés, J.M., Duval, M., Cáceres, I., Harichane, Z., van der Made, J., Pérez-González, A., Abdessadok, S., Kandi, N., Derradji, A., Medig, M., Boulaghraif, K., Semaw, S., 2018. 1.9-million- and 2.4-million-year-old artifacts and stone tool-cut-marked bones from Ain Boucherit, Algeria. *Science* 362 (6420), 1297–1301.
- Schwarcz, H.P., Grün, R., 1988. ESR dating of level L2/3 at La Micoque, dordogne (France): excavation of debénath and rigaud. *Geoarchaeology* 3–4, 293–296.
- Shao, Q., Bahain, J.-J., Falguères, C., Dolo, J.-M., Garcia, T., 2012. A new U-uptake model for combined ESR/U-series dating of tooth enamel. *Quat. Geochronol.* 10, 406–411.
- Shao, Q., Bahain, J.J., Dolo, J.M., Falguères, C., 2014. Monte Carlo approach to calculate US-ESR ages and their uncertainties. *Quat. Geochronol.* 22, 99–106.
- Shao, Q., Chadam, J., Grün, R., Falguères, C., Dolo, J.-M., Bahain, J.-J., 2015. The mathematical basis for the US-ESR dating method. *Quat. Geochronol.* 30, 1–8.
- Stremme, H.E., 1985. Altersbestimmung und Palaoboden in der Quatarstratigraphie. *Bull. Assoc. Fr. Étude Quat.* 2–3, 159–166.
- Tissoux, H., Falguères, C., Voinchet, P., Toyoda, S., Bahain, J.J., Despriée, J., 2007. Potential use of Ti-center in ESR dating of fluvial sediment. *Quat. Geochronol.* 2 (1–4), 367–372.
- Tissoux, H., Toyoda, S., Falguères, C., Voinchet, P., Takada, M., Bahain, J.-J., Despriée, J., 2008. ESR dating of sedimentary quartz from two Pleistocene deposits using Al and Ti-centres. *Geochronometria* 30, 23–31.
- Tissoux, H., Voinchet, P., Lacquement, F., Prognon, F., Moreno, D., Falguères, C., Bahain, J.-J., Toyoda, S., 2012. Investigation on non-optimally bleachable components of ESR aluminium signal in quartz. *Radiat. Meas.* 47 (9), 894–899.
- Toyoda, S., 2015. Paramagnetic lattice defects in quartz for applications to ESR dating. *Quat. Geochronol.* 30, 498–505.
- Toyoda, S., Falguères, C., 2003. The method to represent the ESR signal intensity of the aluminium hole centre in quartz for the purpose of dating. *Adv. ESR Appl.* 20, 7–10.
- Toyoda, S., Voinchet, P., Falguères, C., Dolo, J.-M., Laurent, M., 2000. Bleaching of ESR signals by the sunlight: a laboratory experiment for establishing the ESR dating of sediments. *Appl. Radiat. Isot.* 52, 1357–1362.
- Voinchet, P., Falguères, C., Laurent, M., Toyoda, S., Bahain, J.J., Dolo, J.M., 2003. Artificial optical bleaching of the Aluminium center in quartz implications to ESR dating of sediments. *Quat. Sci. Rev.* 22 (10–13), 1335–1338.
- Voinchet, P., Bahain, J.-J., Falguères, C., Laurent, M., Dolo, J.-M., Despriée, J., Gageonnet, R., 2004. ESR dating of quartz extracted from Quaternary sediments: application to fluvial terraces system of Northern France. *Quaternaire* 15, 135–141.
- Voinchet, P., Toyoda, S., Falguères, C., Hernandez, M., Tissoux, H., Bahain, J.-J., 2015. ESR residual dose in quartz modern samples, an investigation into environmental dependence. *Quat. Geochronol.* 30, 506–512.
- Voinchet P., Falguères C., Pereira A., Nomade S., Biddittu I., Piperno M., Bahain J.-J. (this issue). ESR Dating Applied to Optically Bleached Quartz-A Comparison with ⁴⁰Ar/³⁹Ar Chronologies on Italian Middle Pleistocene Sequences.
- Yokoyama, Y., Falguères, C., Quaegebeur, J.P., 1985. ESR dating of quartz from Quaternary sediments: first attempt. *Nucl. Tracks* 10, 921–928.